VERIZONA PUBLISHER
Publishing Your Ideas

www.verizonaonlinepublishing.com
Vol: 1, Issue: 1

Journal of Robotics and Mechanical Engineering Research

A Novel Equivalent Consumption Minimisation Strategy for a Series Hybrid Electric Vehicle

James McDonald[1], Saber Fallah[2*]

[1] Ford Motor Company, Dunton Technical Centre, Laindon, Basildon, SS15 6EE, UK
[2] Department of Mechanical Engineering Sciences, University of Surrey, UK

***Corresponding author:** Saber Fallah, Department of Mechanical Engineering Sciences, University of Surrey, Guildford, GU2 7XH, UK, Tel: +44-1483-686528; Email: s.fallah@surrey.ac.uk

Article Type: Research, **Submission Date**: 23 February 2015, **Accepted Date:** 12 June 2015, **Published Date:** 19 June 2015.

Citation: James McDonald and Saber Fallah (2015) A Novel Equivalent Consumption Minimisation Strategy for a Series Hybrid Electric Vehicle. J Robot Mech Eng Resr 1(1): 24-30.

Abstract

In this paper, a novel Equivalent Consumption Minimization Strategy (ECMS) is developed for a series hybrid powertrain system, based on the flow of energy through energy sources and components. The performance of the controller is assessed using both urban and highway drive cycles, through comparing results for the series hybrid powertrain system against a comparable conventional powertrain. Fuel economy improvements are achieved by effectively optimizing the distribution of the power generation within the power sources of the system and by promoting battery charging during low-power demand conditions. The simulation results show that the proposed ECMS provides a substantial improvement to fuel economy and energy consumption of a series hybrid electric vehicle, whilst effectively managing battery state of charge.

Introduction

In recent years, there has been a growing trend within the automotive sector for more environmental friendly vehicles due to unsustainable natural resources and growing understanding of the impact of the current transportation fleet on both local and global air quality.

Hybrid Electric Vehicles (HEVs) are considered as more sustainable and cleaner alternatives to current Internal Combustion Engine (ICE) vehicles. Typically, a HEV uses two or more energy sources for power generation, providing greater fuel economy and lower vehicle emissions. However, multiple energy sources introduce the need of a sophisticated control system to optimally distribute the power flow within the energy sources to achieve the desired objectives such as fuel consumption minimization and emission reduction. Different control strategies have been designed so as to fulfill the necessary instantaneous power demand of the vehicle, whilst the State of the Charge (SOC) and overall fuel consumption are managed to meet the overall energy demands of the journey. In general, current power management control systems can be classified as rule-based and optimization-based strategies. Rule-based control strategies work by considering set regions of vehicle performance and using predetermined operation modes to function within these regions, such as pure electric operation, pure ICE operation, hybrid drive and kinetic energy recuperation.

As rule-based strategies are not able to adapt to changing driving behaviors, fuel economy and vehicle emission improvements do not transfer between different drive cycles, thus limiting the application of rule-based strategies to a specific driving cycle. In contrast, optimization-based strategies are often used to overcome this problem through continuously adjusting power generation based upon current vehicle demands, thereby allowing for robust improvements to fuel economy and vehicle emissions reduction in different driving cycles [1].

Equivalent Consumption Minimization Strategy (ECMS) is known as one of the most successful optimization-based strategies for power management of HEVs. Originally, ECMS was developed for parallel HEVs and its effectiveness on parallel-hybrid powertrains has been widely investigated [2-5]. The ECMS was developed based on the idea that discharging the battery at any time is equivalent to some fuel consumption in the future and vice-versa. However, it has been reported in [6] that ECMS might cause significant wheel-torque oscillation due to instantaneously adjusting the power sources being used, thereby affecting system stability. It also might cause the potential for a delayed torque response during initiation of alternative power source, thereby reducing drivability and passenger comfort. These issues can be mitigated or even eliminated in a series or a parallel-series hybrid powertrain, because of decoupling engine power from the road load within these powertrain architectures [6].

Recently, ECMS has been modified and applied to different hybrid powertrain architectures. For instance, Zhang and Vahidi [7] modified the ECMS algorithm by on-line ECMS parameter tuning using partial route preview information. Liu and Peng [8] developed an ECMS with kinematic constraints for a power-split hybrid powertrain while He *et. al.* [9] proposed an adaptive ECMS for such hybrid powertrains using predictive traffic information. Wang *et. al.* [10] proposed an adaptive ECMS which can be updated through drive cycle recognition for the power-split hybrid city buses. The application of ECMS on a series hybrid city bus was investigated by [11]. Also ECMS was modified and

applied on a series hybrid powertrain by [12] and [13]. The former improved the ECMS performance with a novel SOC-sustaining approach while the latter compared the ECMS performance with that of engine power smoothing energy management strategy for a series hybrid electric vehicle (SHEV).

This paper focuses on the validation of a novel form of ECMS for a Series Hybrid Electric Vehicle (SHEV) through the use of a backward facing simulation. Compared to the conventional ECMS which considers the torque generation of the power sources, the modified ECMS proposed in this paper is based upon the power flow throughout the powertrain, thereby representing the electrical power provided to the electric motor by the ICE and battery. In order to precisely determine the fuel consumption of the ICE, the power generated by ICE to drive the vehicle and to recharge the battery is included in ECMS formulation.

The structure of the paper is organized as follows. Modification of ECMS section describes an adaption of ECMS for a series HEV. A backward facing model of a series hybrid powertrain is developed in Powertrain modeling section. Next section is devoted to examining the potential benefits of the proposed ECMS on fuel economy enhancement of a SHEV through simulations.

Finally, Final section summarizes the results and conclusions of the conducted work.

Modification of ECMS for a Series Powertrain

A series hybrid powertrain system, as shown in Figure 1, uses a small and reasonably inflexible ICE at near optimum levels. The ICE is connected to a generator to produce electrical energy which is then transferred either to the battery (energy storage) or to the electric motor.

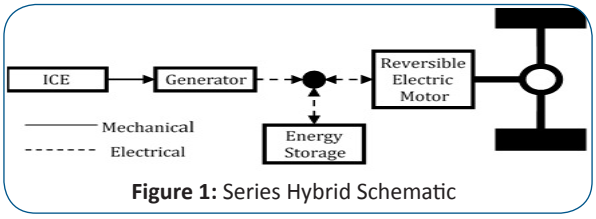

Figure 1: Series Hybrid Schematic

In original ECMS developed for parallel HEVs, the energy flowing through the components is related to the associated mass flow rate of fuel which is a function of provided torques by the ICE and electric motor. Thus, based upon the flow of energy through the ICE, electric motor and battery, the equivalent cost of usage, D_t, is calculated as:

$$D_t = \dot{m}_{ICE}\left(T_{ICE}(t)\right) + \dot{m}_{b,eq}\left(T_{EM}(t)\right) \quad (1)$$

Where the torques provided by the ICE and electric motor are denoted by T_{ICE} and T_{EM}, respectively. The mass flow rate of fuel through the ICE is $\dot{m}_{b,eq}$, whereas the equivalent fuel flow rate through the battery, related to depleted electrical charge is. The equivalent fuel flow rate of the battery was given by [1]:

$$\dot{m}_{b,eq}(t) = \left(s_{dis}\,\alpha\frac{1}{\eta_b\eta_{EM}} + s_{chg}(1-\alpha)\eta_b\eta_{EM}\right)\frac{P_{EM}}{H_{LHV}} \quad (2)$$

Where s_{dis} and s_{chg} are the two equivalence factors for promoting discharging and charging and were used to tune the ECMS to provide appropriate use of the ICE, electric motor and battery of the vehicle under consideration. The efficiency of the battery and electric motor are shown by η_b and η_{EM}, respectively. The power produced by the electric motor is given by p_{EM} and the fuel's lower heating value is denoted by p_{LHV}. Also, α was used to show whether the electric motor is charging or discharging and was calculated as:

$$\alpha = \frac{1+sign\,(T_{EM})}{2} \quad (3)$$

Since conventional ECMS is based upon the torque provided by the ICE and electric motor, this method is no longer suitable for a SHEV in which just the electric motor drives the vehicle. Therefore, it is necessary to modify the equivalent cost, D_t, by considering that the ICE provides power to the electric motor through a generator. In order to determine the equivalent cost of electrical power used to drive the electric motor, an approach considering the power demand of the electric motor from the battery and ICE via the generator is proposed in this paper. To provide an accurate representation of energy flow through the vehicle, the fuel flow rate associated with the ICE is calculated based upon the possibility of providing the power to drive the vehicle and recharge the battery via load point shifting. Load point shifting refers to the case where the ICE is used to operate within its high efficiency region by producing surplus power to recharge the battery. The energy conversion losses in the system are represented by efficiency terms for the battery and generator. Due to the flow of energy through a SHEV, Eq. (4) is developed in order to calculate the equivalent cost of a given power distribution, while Eqs.(5) to (8) are developed to determine the power required by the ICE and the equivalent fuel flow rate of the battery. The equivalent cost of usage is based upon the power flow into the electric motor by the battery and generator. The equivalency constants s_{dis} and s_{chg} are used to determine the cost of battery drive or battery charging respectively, thus through tuning these variables the response of the system can be modified.

$$D_t = \dot{m}_{ICE}\left(P_{ICE,req}(t)\right) + \dot{m}_{b,eq}\left(P_b(t)\right) \quad (4)$$

$$P_{ICE,req}(t) = \left(\frac{P_{ICE,drive}(t)}{\eta_g} + s_{chg}\eta_b\eta_g P_{ICE,charge}(t)\right) \quad (5)$$

$$\dot{m}_{b,eq}(t) = \frac{s_{dis}\,P_b}{\eta_b H_{LHV}} \quad (6)$$

$$P_{demand}(t) = \frac{P_w(t)}{\eta_{EM}} = \frac{P_{ICE,drive}(t)}{\eta_g} + \frac{P_b(t)}{\eta_b} \quad (7)$$

$$P_{ICE,charge} = P_{ICE}^{\max\ eff} - P_{demand}\ ,if\ P_{demand} < P_{ICE}^{\max\ eff} \quad (8)$$

Here, the power required by the battery and ICE are represented by p_b and $p_{ICE,\,req}$, respectively. The power produced by the ICE to drive the vehicle and charge the battery is denoted by $P_{ICE,drive}$ and, $P_{ICE,charge}$ respectively. The maximum efficient power of the ICE is shown by P_{ICE}^{maxeff}. The wheel load power is represented by η_g, whilst the associated power demand required by the electric motor is given by and the efficiency of the generator is denoted by . As highlighted by Eq. (8), load point shifting can be used until the overall ICE power exceeds the maximum efficient power output of the ICE. Using Eqs. (4) to (8), a strategy for calculating the optimum power distribution between the ICE and battery can be determined. In order to ensure that the battery is not damaged, it is necessary to limit the SOC to within the allowable

boundaries. A similar approach is also taken to limit the ICE to high efficiency operation. Through assessing all component interactions, ECMS is modified for a SHEV as shown by Eqs. (9) to (13).

While $SoC_{min} \leq SoC\ (t) \leq SoC_{max}$

$$\left[P_b^{opt}(t), P_{ICE}^{opt}(t)\right] = \arg min_{\left[P_B(t), P_{ICE}(t)\right]} D_T \ if\ P_w > 0 \quad (9)$$

$$P_{ICE}^{opt}(t) = 0, P_b^{opt}(t) = P_w \eta_{EM}\ if P_w \leq 0 \quad (10)$$

$$if\ SoC(t) < SoC_{min}$$

$$P_{ICE}^{opt}(t) = P_w, P_b^{opt}(t) = 0\ if\ P_w > P_{ICE}^{\max\ eff} \quad (11)$$

$$P_{ICE}^{opt}(t) = P_{ICE}^{\max\ eff}, P_b^{opt}(t) = 0\ if\ P_w < P_{ICE}^{\max\ eff} \quad (12)$$

$$if\ SoC(t) > SoC_{max}$$

$$P_{ICE}^{opt}(t) = 0, P_b^{opt}(t) = P_w \quad (13)$$

Where the optimum power for the battery and ICE are P_b^{opt} and P_{ICE}^{opt}, respectively. The current SOC, minimum SOC and maximum SOC are given by *SoC*, SoC_{min} and SoC_{max}, respectively. Regenerative braking is calculated by Eq. (10), whereby as a negative torque is required by the drivetrain the power recovered by the electric motor is stored within the battery. SOC limits are used to ensure the battery remains within the appropriate operating window for high efficiency and long cycle life. When the SOC approaches the lower limit, the battery is no longer used as an energy source and the ICE will operate to provide all the necessary drive power. Throughout periods of low SOC, if the maximum efficient output of the ICE is higher than the current power demand, load point shifting is used to recharge the battery. When the SOC exceeds the upper limit, the ICE is no longer used and the battery is depleted to provide the necessary power [1].

Powertrain Modeling

In order to assess the potential of the proposed ECMS, it is necessary for a simulation model to be developed. The two main forms of simulation models are forward facing and backward facing models. The former represents high accuracy of the system at the expense of high computational burden while the latter is simpler and more computational efficient. In a backward facing model, the tractive force at each wheel and consequently the power demand from the powertrain can be calculated using a predefined speed profile of a given drive cycle, thereby making it useful for initial system development and control strategy validation [14-16]. The following subsections explain the details of the developed backward facing model.

Drivetrain

In order to model the drivetrain, Eqs. (14) to (17) are used to determine the required tractive force, .

$$F_x = m_v \ddot{x} + F_d + F_R + F_m \sin\theta \quad (14)$$

Where,

$$F_d = \frac{1}{2}\rho_a \dot{x}^2\ C_d A \quad (15)$$

$$F_m = m_v g \quad (16)$$

$$F_R = 0.01(1 + 0.022\dot{x})F_m \quad (17)$$

Where acceleration and velocity of the vehicle are $\ddot{x}$ and $\dot{x}$, respectively. The drag force, vehicle weight and rolling resistance are represented by F_d, F_m and F_R, respectively. The total vehicle mass is given by m_v, the angle of the inclination is shown by θ, the density of air is denoted by ρ_a, the coefficient of drag is stated as C_d, the frontal area of the vehicle is shown by *A* and acceleration due to gravity is denoted by *g*. Considering the moment provided by the radius of the driven wheels, the total necessary torque provided by the driving wheels is calculated as:

$$T_w = F_x R_w \quad (18)$$

Where T_w and R_w are the tractive torque and radius of the driven wheels, respectively. The necessary torque for the SHEV and conventional vehicle can be calculated using Eqs. (19) and (20) respectively.

$$T_{EM} = \frac{T_w}{\beta_0} + \dot{\omega}_{EM}(I_{EM} + I_0) \quad (19)$$

$$T_{ICE} = \frac{T_w}{\beta_0 \beta_g} + \dot{\omega}_{ICE}(I_{ICE} + \frac{I_0}{\beta_g}) \quad (20)$$

Where, β_0 and β_g are the gear ratios for the final drive and selected transmission gear for the conventional vehicle. $\dot{\omega}_{EM}$ and $\dot{\omega}_{ICE}$ are the angular accelerations of the electric motor and ICE respectively. I_{EM}, I_{ICE} and I_0 are the second moments of inertia for the electric motor, ICE and final drive respectively. It is noted that inertia losses are neglected in the current modelling [17].

Battery

The open circuit voltage (Figure 2) is a simple model of a battery but still accurate enough to represent the most important battery characteristics. In this model, the terminal voltage, V_{bt}, is compared to the internal resistance, R_{bi}, internal voltage, V_{bi}, and resistive load, R_L.

Kirchhoff's voltage law, one has:

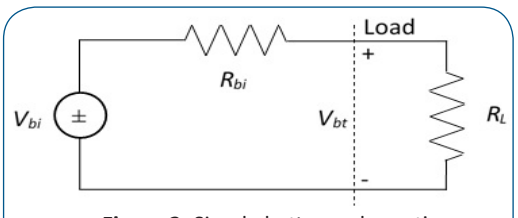

Figure 2: Simple battery schematic

$$V_{bt} + R_{bi} i - V_{bi} = 0 \quad (21)$$

By assuming that the internal resistance is constant and considering the battery power, P_b, and Eq (21), the current variation can be determined as:

$$i = \frac{V_{bi} \pm \sqrt{V_{bi}^2 - 4R_{bi} P_b}}{2R_{bi}} \quad (22)$$

Finally the SOC can then be calculated by comparing the energy available within the battery to the theoretical maximum, E_b, as [1].

$$SOC = \frac{1}{E_b} \int_{t_0}^{t} i(t) V_{bi} \, dt \quad (23)$$

Internal Combustion Engine

In order to reduce computational burden, within the model, the ICE is based upon its characteristic curves. For SHEV modeling, since the ICE is limited to functioning within the highest efficiency region, one dimensional efficiency and fuel flow rate maps are sufficient to be used. However, for the conventional vehicle model, the ICE needs to be used within all areas of operations, with a basic gear selection system implemented to adjust the ICEs output to meet the desired vehicle velocity.

Electric Motor and Generator

Similar to the ICE, representations of the electric motor and generator used within the model are based upon characteristic data of an electric motor. The final drive gear ratio is selected to ensure that the electric motor is able to operate efficiently over the intended drive cycles. Energy conversion losses for both the generator and electric motor are calculated through the use of two dimensional efficiency maps (Figure 3) related to the necessary torque and rotational speed of the relevant component at a given instant. When additional drive is required from the electric motor, the efficiency term is used to calculate the increased power demand required to meet the given speed profile. In contrast, for both the generator and the electric motor when under braking, the efficiency terms are used to determine the respective cost of the energy conversion and thus the reduced available power after conversion.

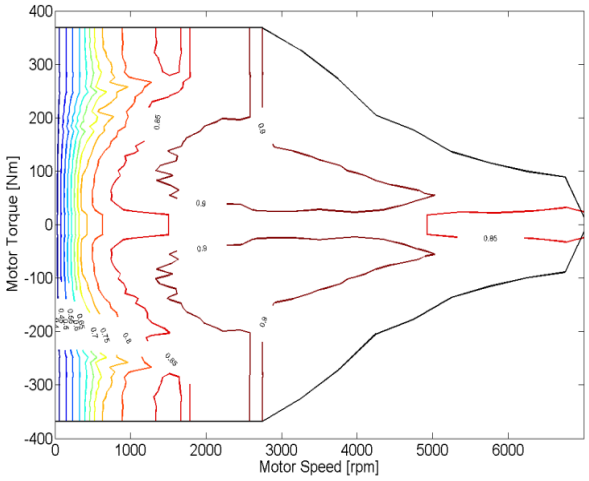

Figure 3: Electric motor (generator) efficiency map

Simulation Results and Discussion

For the simulation purposes, the Federal Test Procedure (FPT-75) and Highway Fuel Economy Driving Schedule (HWFET) drive cycles (Figure (a) and 4(b), respectively) are considered. To demonstrate the potential of ECMS for SHEVs, the controller is

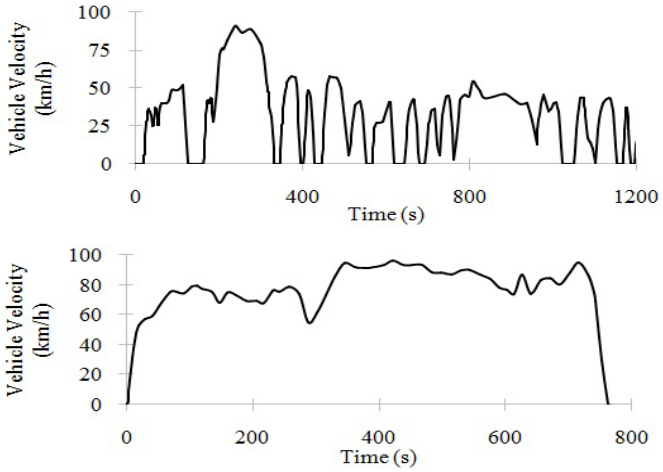

Figure 4: Drive Cycle a) FPT-75 b) HWFET

Table 1: Key Vehicle Variables

Variable	Value	
Driven Wheel, Radius	0.31 m	
Density of Air	1.2 kgm^{-3}	
Coefficient of Drag	0.32	
Frontal Area	2.26 m^2	
Vehicle Mass	1200 kg	
Electric motor, Torque Range	±368 Nm	
Electric motor, Speed Range	±732.9 rads^{-1}	
ICE, Maximum Power	35 kW	
Final Drive Ratio	3.5	
Battery, Total Energy	6.1 kWh	
Battery, Internal Resistance	12.5 µΩ	
Lower Heating Value of Fuel	44 MJ/kg	
Equivalency Discharge Factor	1.25	5.5
Equivalency Charge Factor	-0.3	-1
Battery, Maximum Power	1700	W

separately tuned for each drive cycle, thus enabling SOC to be well maintained and a fair representation of potential fuel economy improvements to be provided. The values used throughout the simulations are summarized in Table 1.

It is noted that due to the different components used within both a SHEV and conventional vehicle, the exact efficiency and fuel consumption for different components will be slightly different than those used within the simulation. However as the ICE and generator used within the SHEV model are restricted to high efficiency regions, in conjunction with other efficiency values throughout the powertrain, the errors produced by these results are neglegible.

The power distribution between the ICE and battery by the proposed ECMS controller for FTP-75 drive cycle is shown

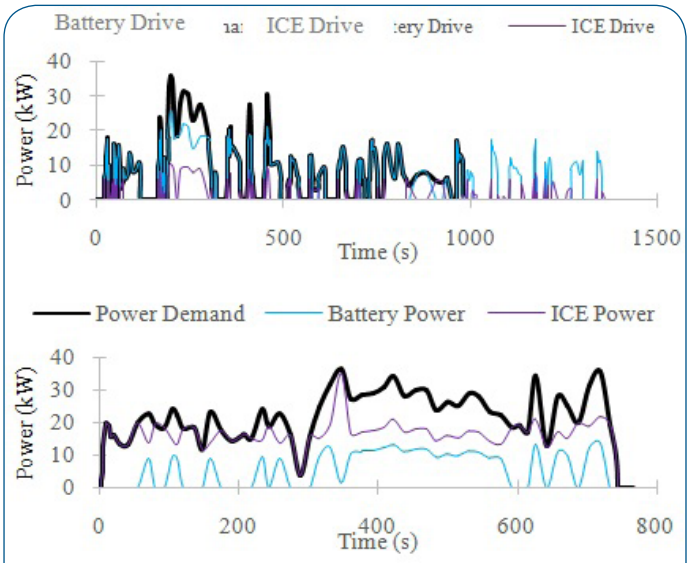

Figure 5: Power distribution throughout a) FPT-75 b) HWFET

in Figure 5(a). As indicated by this figure, the battery highly contributes in providing the required power demand, thus allowing for a significant reduction in fuel consumption. The heavy battery drive is facilitated by kinetic energy recuperation related to the frequent stop/start behavior experienced within this cycle and load point shifting which is implemented for demand equal to and below 5 kW. Throughout periods of high power demand requiring above 20 kW, in order to reduce energy consumption, the ICE is used within high efficiency regions to support battery drive, thus maximizing the operation efficiency. Due to the reduced availability of regenerative braking provided by stop/start driving, the tuning selected for the HWFET cycle favors ICE drive, whereby 74% of the required power is produced by the ICE (Figure 5(b)). During periods of power demand exceeding 20 kW, the battery is used to support drive, enabling the ICE to remain within high efficiency operation, whilst the SOC of the battery is also well maintained.

The power distribution of the ICE is also considered, whereby the amount of the generated power to charge the battery and drive the vehicle are compared, as shown in Figure 6. As can be seen in Figure 6(a), load point shifting is experienced throughout the FPT-75 cycle, whereby sharp peaks of ICE charge above 30 kW are observed in conjunction with low ICE power of approximately 5 kW, thus allowing for the ICE to operate at the maximum efficient output. Load point shifting is only seen in these areas due to low power demand promoting ICE drive. As mentioned previously, this form of power fluctuation can reduce drivability through instability for parallel HEVs, however this problem is minimized for SHEVs as ICE power is decoupled from the road load. Increased ICE power generation is also seen across the HWFET cycle (Figure 6(b)), however, due to the greater use of ICE power, total power production by the ICE no longer experiences sharp peaks and troughs seen in the FPT-75 cycle, alternatively ICE use is maintained within the high efficiency and high power regions of operation throughout the majority of the cycle. As mentioned previously, the HWFET cycle exposes the vehicle to extended periods of high velocity driving, thus requiring above 20 kW of power, throughout these periods to achieve maximum power, the battery is used in unison with the ICE and the load point shifting is no longer utilized.

In the powertrain model, a 6.1 kWh battery is considered, with an initial SOC of 60% and with operation limit of 40% to 80%. As Figure 7 shows, during the two considered drive cycles the power provided to the battery, either via kinetic energy recuperation or load point shifting is converted into a positive current which is used to charge the battery. During the initial stages of the highly urban FPT-75 cycle a high continuous power demand is required and as such the battery is depleted to provide drive (Figure 7(a)). Throughout the remainder of the cycle a lower power demand is required, hence although the battery is continually utilized to drive the vehicle kinetic energy recuperation experienced during the latter stage of the cycle enables the SOC to be increased. For the HWFET (Figure 7(b)), as minimal kinetic energy recuperation is experienced, the SOC of the battery is increased predominately by load point shifting. During the initial portion of the cycle, the required power is all provided by the ICE, in addition to this load point shifting is implemented until 300 s, increasing the SOC to 73%. After this stage of the cycle, a sustained period of greater than 20 kW power demand is experienced where the battery is used to support the ICE, and therefore reducing the current SOC. Although current variation is experienced across both

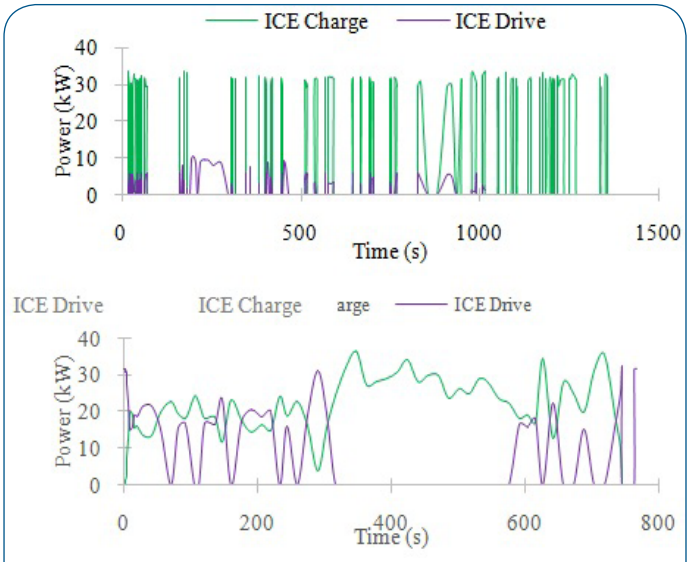

Figure 6: ICE Power Distribution throughout a) FPT-75 b) HWFET

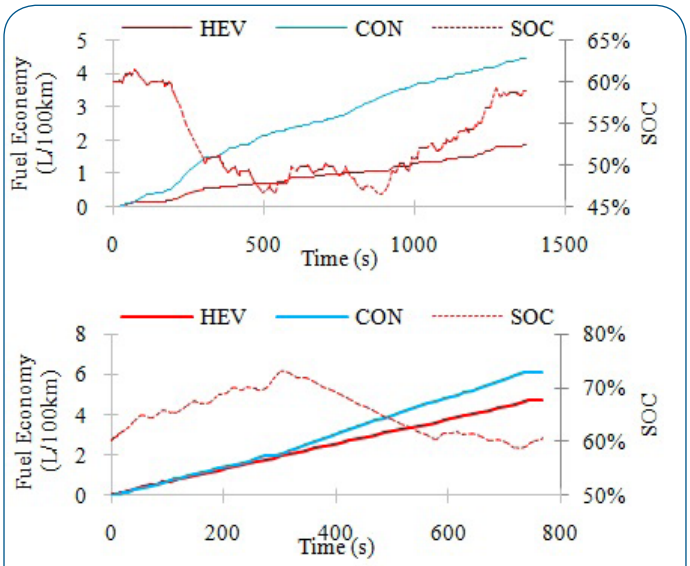

Figure 7: Fuel consumption and SOC variation a) FPT-75 b) HWFET

drive cycles, the overall SOC variation does not exceed 15%, thus suggesting that a properly tuned ECMS is able to provide effective use of the provided battery, allowing for suitable battery life. Also Figure 7(a) shows a 59% lower fuel consumption for the SHEV compared to a conventional vehicle over FTP-75. The significant improvement in fuel economy is due to the large of amount of kinetic energy which could be recovered and then utilized by the electric motor. A fuel economy improvement of 23% is achieved for the SHEV compared to the conventional vehicle during the HWFET (Figure 7(b)), whereby as discussed the use of load point shifting during the early stages of the cycle, enabled battery drive to be effectively implemented during periods of high power demand. As it is necessary with the developed form of ECMS to provide the achieved improvements with different ECMS tuning, it would be beneficial for an adaptive approach to be applied, allowing for broader use of the developed strategy. By

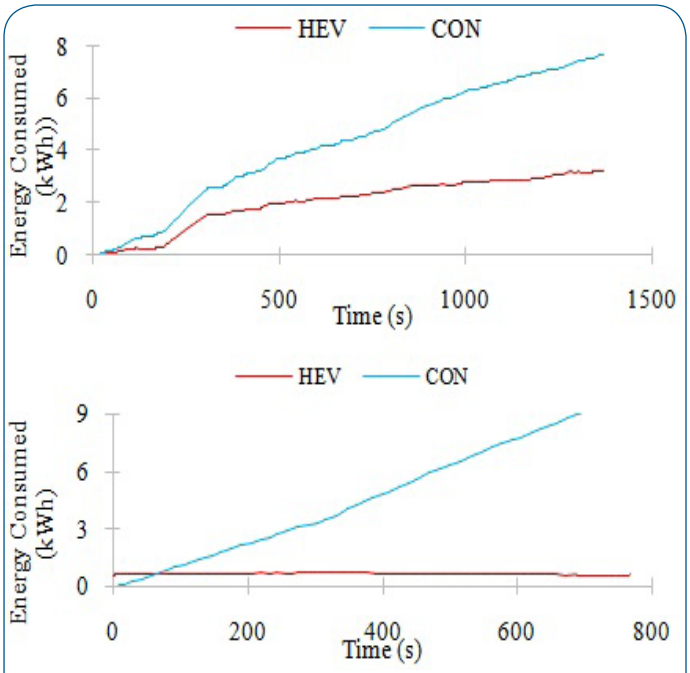

Figure 8: Energy Consumption throughout a) FPT-75 b) HWFET

combining the generated energy from the fuel with the change in stored energy of the battery, the overall energy consumption of the SHEV is studied against that of the conventional vehicle in Figure 8. As can be seen from this figure due to the use of load point shifting and kinetic energy the SHEV consistently consumes less energy. Whereby during the FPT-75 and HWFET drive cycles energy consumption is reduced by 58% and 24% respectively. As SOC is well maintained during both cycles, the reduction in total energy consumption is directly comparable with the improvements seen for fuel economy.

In the above mentioned simulation results, equivalency values have been selected separately for each drive cycle to demonstrate the maximum achievable fuel economy improvements for both urbanized and highway driving, whereby, for the FPT-75, and are set equal to 1.25 and -0.3, respectively. A negative value for is required to promote battery charging as additional fuel is needed during load point shifting due to the surplus power produced. Figure 9 indicates the sensitivity of the proposed ECMS against a ±20% change in in terms of variation in SOC and energy consumption for the FPT-75 drive cycle. As shown, an increase in reduces battery drive and as such encourages SOC increase

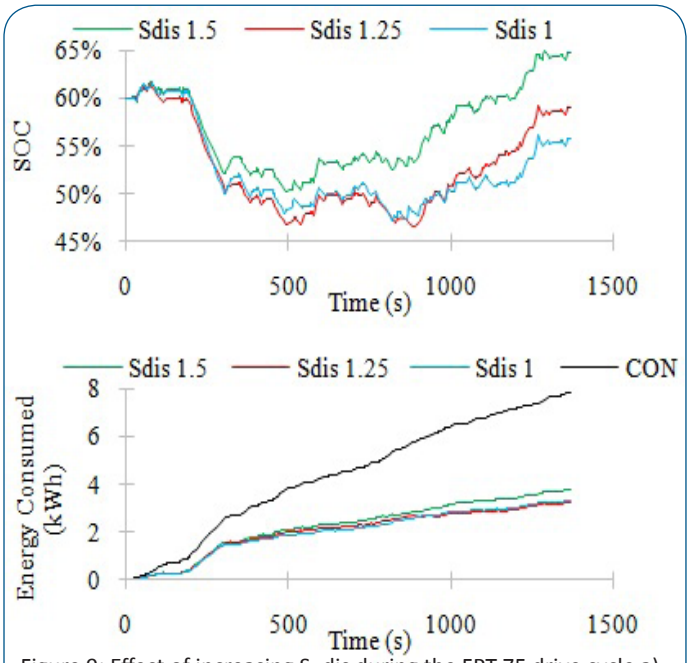

Figure 9: Effect of increasing S_dis during the FPT 75 drive cycle a) SOC b) Energy consumption

and ICE drive, ultimately causing a slight increase in energy consumption. In contrast, a reduction in encourages battery drive, reducing fuel consumption and battery SOC.

Conclusion

In this paper a novel modification of ECMS was proposed for a series HEV and assessed, via a backward facing simulation, against FPT-75 and HWFET drive cycles. The simulation results indicated that the proposed ECMS is able to provide substantial improvements to a series HEV both in terms of overall fuel and energy consumption. Fuel and energy consumption improvements are achieved through the effective selection of load point shifting during periods of low power demand, which is also supported by kinetic energy recuperation during urban driving.

Nomenclature

i:	Battery current
$\dot{m}_{ICE}$:	Engine fuel rate
$\dot{m}_{b,eq}$:	Equivalent battery fuel rate
s_{chg}:	Charging equivalent factor
s_{dis}:	Discharging equivalent factor
E_b:	Nominal energy capacity of the battery
H_{LHV}:	Fuel lower heating value
I_{EM}:	Second moment inertia of electric motor
I_{ICE}:	Second moment inertia of engine
I_o:	Second moment inertia of final drive
P_{ICE}:	Engine power
P_{EM}:	Electric motor power
R_w:	Radius of the driven wheel
R_{bi}:	Internal battery resistance
SOC:	Battery state of the charge
T_{ICE}:	Engine torque
T_{EM}:	Electric motor torque
T_w:	Tractive torque
V_{bt}:	Battery terminal voltage
V_{bi}:	Battery voltage
β_o:	Final drive gear ratio

β_g:	Transmission gear ratio
$\dot{\omega}_{ICE}$:	Angular acceleration of engine
$\dot{\omega}_{EM}$:	Angular acceleration of electric motor
η_b:	Battery efficiency
η_{EM}:	Electric motor efficiency

References

1. Khajepour A, Fallah S, Goodarzi A. Electric and hybrid vehicles: Technologies, Modeling and Control: A Mechatronic Approach. NJ: John Wiley & Sons Ltd; 2014.

2. Paganelli G, Guerra TM, Delprat, J-J Santin S, Delhom M, Combes E. Simulation and assessment of power control strategies for a parallel hybrid car. Proc. of the Inst. of Mechanical Engineers, Part D: J. of Automobile Engineering. 2000; 214(7):705-717. doi: 10.1243/0954407001527583.

3. Paganelli G, Delprat S, Guerra T, Rimaux J, Santin J. Equivalent consumption minimization strategy for parallel hybrid powertrains. Vehicular Technology Conference. 2002; 4:2076–2081. doi: 10.1109/VTC.2002.1002989.

4. Sciarretta A, Back M, Guzzella L. Optimal control of parallel hybrid electric vehicles. IEEE Trans. on Control Systems Technology. 2004; 12(3):352-363. doi: 10.1109/TCST.2004.824312.

5. Musardo C, Rizzoni G, Guezennec Y, Staccia B. A-ECMS: An Adaptive Algorithm for Hybrid Electric Vehicle Energy Management. European J. of Control. 2005; 11(4-5). doi:10.3166/ejc.11.509-524.

6. Schacht EC, Bezaira B, Cooley B, Bayar K, Kruckenberg JW. Addressing Drivability in an Extended Range Electric Vehicle Running an Equivalent Consumption Minimisation Strategy (ECMS). SAE International. 2011. doi: 10.4271/2011-01-0911.

7. Zhang C, Vahidi A. Route Preview in Energy Management of Plug-in Hybrid Vehicles. IEEE Trans on Control Systems Technology. 2012; 20(2):546-553. doi: 10.1109/TCST.2011.2115242.

8. Liu J, Peng H. Modeling and control of a power-split hybrid vehicle. IEEE Trans on Control Systems Technology. 2008; 16(6): 1242-1251. doi: 10.1109/TCST.2008.919447.

9. He Y, Chowdhury M, Pisu P, Ma Y. An energy optimization strategy for power-split drivetrain plug-in hybrid electric vehicles. J. of Transportation Research Part C 22. 2012; 22:29-41. doi:10.1016/j.trc.2011.11.008.

10. Wang J, Wang Q, Wang P, Zeng X. The development and verification of a novel ECMS of hybrid electric bus. Mathematical Problems in Engineering. 2014; 2014(2014): 14. doi: http://dx.doi.org/10.1155/2014/981845.

11. Xu L, Cao G, Li J, Yang F, Lu L, Ouyang M. Equivalent consumption minimization strategies of series hybrid city buses. In: Francisco Macia Perez, editor. Energy Management. 2010.

12. Sezer V, Gokasan M, Bogosyan S. A novel ECMS and combined cost map approach for high-efficiency series hybrid electric vehicles. IEEE Trans on Vehicular Technology. 2011; 60(8):3557-3570. doi: 10.1109/TVT.2011.2166981.

13. Di Cairano S, Liang W, Kolmanovsky IV, Kuang ML, Phillips AM. Engine power smoothing energy management strategy for a series hybrid electric vehicle. American Control Conference; 2011 July29; San Francisco, CA. p. 2101-2106.

14. Watanabe K, Tani M, Yamamuro T, Kubo M. Development of Integrated Powertrain Simulation for Hybrid Electric Vehicles Considering Total Energy Management. SAE International. 2012. 10.4271/2012-01-1012.

15. Katrasnik T. Analysis of Fuel Consumption Reduction Due to Powertrain Hybridization and Downsizing of ICE. SAE International. 2006. doi: 10.4271/2006-01-3262.

16. Prachar T, Poltenstein A, Magerl L, Winter S, Gerhard L, Caldevilla A, et al. Consideration of Different Hybrid Powertrains with the Help of a Model in Longitudinal Dynamics Using DymolaTM. SAE International. 2006. doi: 10.4271/2006-01-1126.

17. Rizoulis D, Burl J, Beard J. Control Strategies for a Series-Parallel Hybrid Electric Vehicle. SAE International. 2001. doi: 10.4271/2001-01-1354.